Scaling of magnetization and some basic parameters of $Ba_{1-x}K_xBiO_{3+y}$ superconductors near T_c

S. N. Barilo, S. V. Shiryaev, and V. I. Gatalskaya
Institute of Physics of Solids and Semiconductors, Academy of Science, Minsk 220072, Belarus

J. W. Lynn
Center for Superconductivity Research, University of Maryland, College Park, Maryland 20742
and NIST Center for Neutron Research, National Institute of Standards and Technology, Gaithersburg, Maryland 20899

M. Baran, H. Szymczak, and R. Szymczak
Institute of Physics, Polish Academy of Science, Warsaw PL 02-668, Poland

D. Dew-Hughes
Department of Engineering Science, Oxford University, Oxford OX1 3PJ, United Kingdom
(Received 10 June 1998)

Reversible magnetization and hysteresis loops have been studied over wide ranges of magnetic field and temperature for single crystals of $Ba_{1-x}K_xBiO_{3+y}$ ($x=0.34$, 0.37, 0.41, and 0.46). The main goals were to derive critical parameters of superconductors with a cubic structure as well as to explain the origin of flux pinning and peak (fishtail) effect observed in all samples. Values of the electron-phonon interaction constant of $\lambda_{ph}\sim 1$, ~ 0.76, and 0.9 for $Ba_{1-x}K_xBiO_{3+y}$ with $x=0.34$, $x=0.37$, and $x=0.41$, respectively, have been obtained. The data show that this family belongs to oxide superconductors with at least an intermediate strength of coupling. The pinning force density has been scaled into a single curve for wide field and temperature ranges. The functional form of the scaling curve reflects various mechanisms of flux pinning. For $Ba_{0.54}K_{0.46}BiO_{3+y}$ the peak effect is mainly due to a dynamical contribution. However, the fishtail for $Ba_{1-x}K_xBiO_{3+y}$ with $x=0.34$, 0.37, and 0.41 has its origin in the crossover between two pinning mechanisms induced by external magnetic field and/or temperature. For the $Ba_{0.59}K_{0.41}BiO_{3+y}$ crystal a seeded growth-induced anisotropy was found to be responsible for differences in low-field susceptibility and in hysteresis loops observed for different magnetic-field orientations. [S0163-1829(98)00442-1]

I. INTRODUCTION

Despite intense interest in such a promising compound like the isotropic superconductor $Ba_{1-x}K_xBiO_y$ (BKBO) the question of the mechanism responsible for superconductivity at $T_c\sim 30$ K and of the magnitude of the coupling constant remains open. Experimental studies to determine the energy gap value Δ_0, the isotopic coefficient α, and the electron-phonon interaction constant λ_{ph} are known to provide very important information for the solution of this problem. For conventional weak-coupling BCS superconductors the constant $2\Delta_0/k_BT_c$ has the value of 3.53,[1] while for BKBO the value determined from a superconductor–insulator–normal-metal (SIN) configuration of tunneling measurements[2–7] ranges from 3.7 to 4.1 indicating intermediate to strong coupling. Experimentally determined critical parameters of BKBO superconductors obtained by different authors for single crystals, ceramics, and films are listed in Table I. As can be seen, the results of measurements of thin BKBO films in the high-frequency[19] and IR Ref. 16 ranges agree well with the findings of tunneling measurements of Δ_0 and again indicate also the intermediate character of coupling in this compound.

The early observation of the isotope effect in BKBO (Ref. 10) yielded fairly conflicting results. The theoretical value of the isotopic coefficient $\alpha = d\ \ln T_c/d\ \ln m$ in BCS superconductors is $\frac{1}{2}$,[27] assuming that neither Coulomb interaction nor anharmonic optical modes are present. In Refs. 10, 28, and 29 α values were determined to be 0.20, 0.4, and 0.42, respectively, while in a recent paper[23] an influence of potassium concentration on α in the $Ba_{1-x}K_xBiO_3$ compounds has been found. The authors found that the isotopic coefficient α increases with the decreasing potassium concentration [$\alpha = 0.21$ ($x=0.45$), 0.26 ($x=0.375$), and 0.34 ($x=0.36$)], while the energy-gap values $2\Delta_0/\kappa_bT_c$ vary from 4.0 ($x=0.45$) to 4.5 ($x=0.375$), and 4.8 ($x=0.36$). Accordingly, the coupling-constant estimations λ_{ph} are 1 ($x=0.45$), 1.45 ($x=0.375$), and 1.80 ($x=0.36$), respectively,[23] and indicate strong coupling. These results are connected with the conclusions[30] about the growth of the coupling constant λ_{ph} as the potassium concentration approaches the superconductor-insulator boundary ($x\sim 0.35$).

From investigations of transport properties of BKBO crystals[9] the coupling-constant value $\lambda_{ph}=1.7-2.1$ was determined, arguing that BKBO cannot be treated as a conventional weakly coupled superconductor. The value $\lambda_{ph}=2$ has been obtained from dynamic susceptibility measurements on superconducting BKBO powder.[26] However, in Ref. 14 the electron-phonon interaction parameter calculated from the magnetic and resistivity measurements of critical parameters of $Ba_{0.62}K_{0.38}BiO_3$ single crystals was 0.48–0.96. From the examination of the structure phase diagram of $Ba_{1-x}K_xBiO_3$ calculations of the constant of electron-phonon interaction for $0\leqslant x\leqslant 0.5$ were made[20] and revealed a correlation of λ_{ph}

TABLE I. Critical parameters of $Ba_{1-x}K_xBiO_3$ superconductors from different experiments.

$H_{c1}(0)$ (Oe)	$H_{c2}(0)$ (T)	$-dH_{c2}/dt$ (T/K)	λ_L (Å)	ξ (Å)	κ	γ (mJ/mol K^2)	$2\Delta_0/kT$	λ_{ph}
8[a] (Ref. 8)	32[b] (Ref. 9)	~0.5[a,b] (Refs. 9 and 10)	803[a] (Ref. 8)	51[a,b] (Ref. 11)	50[a,b] (Ref. 11)	2.4[a,b] (Ref. 11)	3.5[b] (Ref. 12)	~1[b] (Ref. 3)
35[a] (Ref. 13)	16–21[b] (Ref. 14)	0.57[b] (Ref. 11)	2200[a] (Ref. 13)	46[c] (Ref. 15)	59[a] (Ref. 13)	1.5[a] (Ref. 10)	3.5[b] (Ref. 16)	0.1[b] (Ref. 17)
100[b] (Ref. 11)	15.4[a] (Ref. 8)	0.78[c] (Ref. 15)	2500[b] (Ref. 11)	36.8[a] (Ref. 13)	21[a] (Ref. 8)	0.3[a] (Ref. 18)	3.8[c] (Ref. 19)	0.9[a] (Refs. 20 and 21)
95[b] (Ref. 14)	17.3[a] (Ref. 13)	0.52[b] (Ref. 17)	2700[b] (Ref. 14)	32[b] (Ref. 9)	60–68 (Ref. 14)	3.4[a] (Ref. 21)	3.7–4[b,c] (Refs. 2–7)	1.7–2.1[b] (Ref. 9)
400[b] (Ref. 22)	12.6[b] (Ref. 11)	0.87[a] (Ref. 13)	3300[c] (Ref. 19)	45.3[a] (Ref. 8)		2.36[a] (Ref. 13)	4.1[b] (Ref. 7)	1–1.18[b] (Ref. 23)
	15.2[c] (Ref. 15)	0.78[b] (Ref. 14)	3400[c] (Ref. 24)	39–45[a] (Ref. 14)		2.31[b] (Ref. 14)	4–4.8[b] (Ref. 23)	0.48; 0.96[b] (Ref. 14)
	>25[b] (Ref. 25)	0.9[a] (Ref. 8)						2[a] (Ref. 26)
								1[b] (Ref. 12)

[a]Ceramics.
[b]Single crystals.
[c]Thin and thick films.

values with the experimental dependence of $T_c(x)$.[30] To illustrate, for potassium content $x=0.4$, $\lambda_{ph}=0.95$.[20] Thus, we believe that BKBO can be considered as a conventional BCS superconductor with intermediate coupling. However, the coupling constant $\lambda_{ph}=0.35$ determined in Ref. 17 also supports the assumption of weak coupling in this material, which runs counter to the findings given in Ref. 21, where λ_{ph} was estimated from the specific-heat measurements for the $Ba_{1-x}K_xBiO_3$ ceramic sample to be of 0.9, and corresponds to intermediate coupling. The calculation[31] of thermodynamic properties of $Ba_{0.7}K_{0.3}BiO_3$ in terms of the Eliashberg theory on the assumption of an electron-phonon interaction gives the following values: $2\Delta_0/k_BT_c=4.15$ and $\lambda_{ph}=1.18$, i.e., this superconductor possesses strong coupling (Table I and references cited therein).

The magnetic-field penetration depth λ_L is an exceptionally important characteristic of a superconductor and its temperature dependence $\lambda_L(T)$ is very sensitive to the character of the coupling. In some papers concerned with measurements of the $\lambda_L(T)$ by the muon-spin-rotation technique[24] and resonant measurement in the high-frequency range,[19] it was shown that BKBO is a weakly coupled BCS superconductor with $\lambda_L(0)=3300-3400$ Å. One way of determining the temperature dependence of $\lambda_L(T)$ is measurement and analysis of reversible magnetization isotherms $M(H)$ in the intermediate magnetic fields range $H_{c1}\leqslant H\leqslant H_{c2}$. In this region the following relationship between the magnetization and the magnetic field is valid for high-T_c superconductors:

$$-4\pi M(T,H)=\frac{\phi_0}{8\pi\lambda_L^2(T)}\ln\frac{\eta}{l}\left[\frac{H_{c2}(T)}{H}\right]-\frac{4\pi k_BT}{\phi_0C\xi(T)}\ln\frac{16\pi k_B\lambda_L^2(T)}{\alpha\phi_0\xi^3(T)H\sqrt{e}}, \quad (1)$$

where the first term describes the London regime with the linear $M(H)$ dependence,[32] and the second part arises as a result of thermodynamic fluctuations,[33] ϕ_0 is the magnetic flux quantum, and η/l, α, C are constants of the order of unity that depends on the structure of the vortex lattice; ξ is the coherence length. It is recognized that thermodynamic fluctuations in high-T_c cuprates can affect significantly the field dependence of magnetization and make a distinct contribution of the fluctuations into the $M(H)$ behavior at high temperatures.[34] The temperature range $\Delta T=GT_c$, where fluctuations effects are observable, is determined by the Ginzburg parameter G, estimated for BKBO crystals previously as $\sim 3\times10^{-4}$ to be markedly lower than one for cuprates with the order of $G=10^{-2}-10^{-3}$.[35] So, the use of a shortened first term of Eq. (1) in analyzing the BKBO magnetization data at temperatures near T_c is quite justified. The constant η/l vanishes under differentiation of the first part of expression (1) with respect to $\partial \ln H$:

$$\frac{\partial M}{\partial \ln H}=\frac{\phi_0}{32\pi^2\lambda_L^2(T)}. \quad (2)$$

Relation (2) for accessible magnetic fields is usually applicable in a limited temperature range close to T_c for an isotropic superconductor free of vortex-lattice pinning. One can determine the slope $dM/\ln H$ and hence the magnetic-field

penetration depth λ_L for various temperatures and analyze $\lambda_L(T)$ in terms of the mechanism of pairing. In our previous paper[36] a preliminary estimation of λ_L for BKBO single crystals has been given. In this work we have carried out systematic investigations of reversible magnetization $M(H)$ isotherms near T_c on the same single crystals with the aim of determining the temperature dependence $\lambda_L(T)$, critical fields, and other Ginzburg-Landau parameters. The heat-capacity jump, corresponding to the superconducting transition of the BKBO crystal, and the constant of electron-phonon interaction are also estimated (Sec. III A).

Exploration of the temperature and field dependencies of the bulk pinning force density F_p, defined as $|J_c B|$,[37] is a particularly advantageous method for analysis of the pinning mechanism in superconductors. The pinning force scaling $F_p(b)$, where $b=B/B_c$ (B_{c_2}, the upper critical field), is generally examined in conventional Nb_3Sn superconductors, since the functional form $F_p(b)$ has frequently allowed conclusions to be drawn about the nature of pinning in the material. This asymptotic expression for the bulk pinning force has been first derived in Ref. 38 for niobium alloys:

$$F_p = \text{const} \times [B_{c_2}(T)]^{2.5} f(b), \tag{3}$$

where $f(b)$ depends only on the normalized magnetic field. To put it differently, the knowledge of F_p and $f(b)$ for a hard superconductor at temperature T_1 permits one to obtain F_p at any fixed temperature T_2. In Ref. 37 the possibility of the flux-creep effect on the scaling F_p has been dealt with to show that it can be ignored in the case of hard superconductors. Campbell and Evetts,[39] as well as Dew-Hughes,[40] have demonstrated that in conventional hard superconductors the pinning force density F_p by and large can be represented as

$$F_p = F_{p_0}(T) b^p (1-b)^q, \tag{4}$$

where $p<q$ depends on (i) the defect dimensionality (point, two-dimensional, or bulk), (ii) the type of interaction (core pinning or magnetic pinning), and (iii) the nature of pinning center (normal or superconducting). According to Kramer's theory, based on the vortex-lattice shear model, the pinning force follows expression (4) while the coefficients p and q depend on the elastic properties of the vortex lattice and at large b value $f(b) \sim (1-b)^2$.[41] The deviation from the scaling law for $F_p(4)$, in turn, with changing temperature and magnetic field can be related to the effects decaying the asymptotic behavior $F_p(b)$, for instance, the flux-creep effect and matching effect specified by commensurability of the vortex-lattice period and crystal microstructure, as well as of the various nature and size of pinning centers.[39]

A number of studies on the scaling F_p in LaSrCuO,[42,43] YBaCuO,[44–52] BiSrCaCuO,[51,53] and TlBaCuO (Ref. 54) have been reported. A high-temperature superconductor (HTSC) is distinguished from a conventional hard superconductor by high values of T_c, short coherence length, large spatial anisotropy, and lower activation energy of pinning. This also influences the pinning force scaling law F_p as the critical current and bulk pinning force decrease to zero with the irreversibility field B_{irr} which is much lower than B_{c_1}. A set of fields $B_{\text{irr}}(T)$ constitutes scaling fields for HTSC materials, and the scaling law for the bulk pinning force is

$$F_p(b',T) = F_{p_0}(T) f(b') = F_{p_0}(T) b'^p (1-b')^q, \tag{5}$$

where $b' = B/B_{\text{irr}}(T)$.

In the majority of HTSC materials over a broad range of external fields the above-mentioned scaling F_p has been observed. However, the exponential fall of magnetization with increasing magnetic field is frequently seen at large fields, i.e., the term $1-b'$ in Eq. (5) on this section of the phase diagram B-T should be replaced by $b\exp(-b/b')$. In this connection, the conclusion has been drawn that one should not expect a perfect scaling F_p for high-T_c superconductors in so far as the effect of the flux creep and flux flow cannot be neglected.[55] At elevated temperatures, $F_p(B,T)$ is determined not only by the critical current density in the absence of activation process $J_{c_0} = F_{p_0}/B$, but also by the activation energy $u(\gamma,B,T)$. Alternatively, in the low-temperature range the flux creep is insignificant. In some HTSC compounds, for instance in the overdoped LaSrCuO,[50] F_p does not obey Kramer's scaling law.[42] The pinning force density scaling law of the $Ba_{1-x}K_xBiO_{3+y}$ (BKBO) superconductor with $T_c \approx 30$ K, which are intermediate between conventional and layered high-T_c superconductors, is not understood yet. These compounds feature a simple-cubic structure, along with the absence of CuO_2 phases and magnetic ions in the lattice. We have first seen and studied comprehensively the peak effect in magnetization for BKBO single crystals with $x \geqslant 0.33$.[36] The peak $F_{p\,\max}(H)$ shifts to the upper-field range with the temperature decreasing while its value rises. The value of the normalized pinning force $F_p/F_{p\,\max} = f(H/H_{\max})$ is scaled to a single curve up to $H_{\max}$ for all the measured isotherms. However, the scaling was disrupted at higher fields.

In this paper we report on a comprehensive study of the field dependence of the bulk pinning force F_p for BKBO single crystals with various potassium concentration, and of the scaling law in dependence of temperature aimed at interpreting the peak effect nature in high-T_c superconductors with isotropic structure (Sec. III B). We have also investigated the effect of seeded growth-induced anisotropy on magnetic properties of BKBO ($x=0.41$) single crystal in superconducting state (Sec. III C).

II. SAMPLES AND EXPERIMENTAL TECHNIQUE

Magnetic measurements were taken from four single crystals of BKBO. The electrodeposition growth method was used for all the samples. The first three crystals, with potassium concentration $x=0.34$, 0.37, and 0.46, respectively, and typical dimensions of $2\times2\times2$ mm^3, were grown by spontaneous crystallization[56] and exhibited $T_c = 19.5$–31 K depending on the potassium concentration. The fourth one, with $x=0.41$, was prepared by the seeded growth technique that allows fairly large crystals up to 2 cm^3 to be grown with $T_c \sim 31$ K and a relatively narrow superconducting transition to be obtained. The fourth sample had approximately cubic shape with dimensions $1.92\times1.90\times1.90$ mm^3 and was cut from a central part of as-grown large crystal ($10\times15\times5$ mm^3). All faces of the sample are oriented (100)-type planes. One of them is the natural growth surface. To reveal any effects related to the growth-induced anisotropy the chemical etching technique has been applied to neighboring

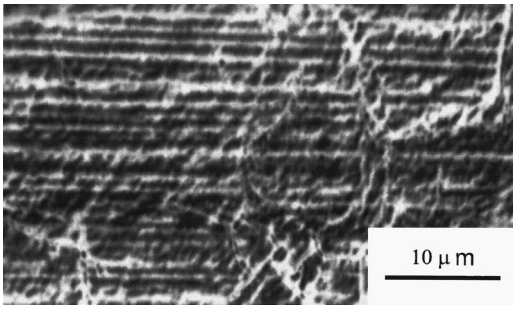

FIG. 1. The stripe defects structure oriented parallel to the natural (001) growth surface of $Ba_{0.59}K_{0.41}BiO_{3+y}$ single crystal was revealed by chemical etching on perpendicular cut of the sample (none could be found on the cut parallel to natural face).

parts of the same crystal. As a result, a stripe structure parallel to the growth surface on faces cut perpendicular to this one was found. No such structure was obtained on faces parallel to the growth surface. The period of etched defects structure was 1–2 μm (Fig. 1). The first indication in microstructure evidence to indicate what might be responsible for the pinning is presented below. As has been mentioned, the sample with $x=0.41$ reveals the seeded growth-induced anisotropy. Small-angle neutron scattering (SANS) was employed to investigate this structure, and the SANS pattern obtained at room temperature is shown in Fig. 2. The experiments were carried out on the NG-7 spectrometer at the NIST Center for Neutron Research, using both moderate and high resolution. These data were taken with a neutron wavelength of 12 Å, no guides, and the two-dimensional position-sensitive detector at a distance of 12 m from the sample. The square-shaped pattern has its corners in the [110] crystallographic direction, and the intensity in any particular direction falls off as $1/Q^4$. This Porod-type scattering indicates that the structural defects producing the scattering are considerably larger than the range explored here, consistent with the optical micrographs that suggest a length scale of ~ 1 μm.

The potassium concentration of all measured samples was determined by three methods: (1) from x-ray measurements of the crystal-lattice parameters according to the calibration curve;[30] (2) from neutron activation analysis; (3) from the measurements of natural radioactivity of the isotope ^{40}K.

The reversible (irreversible) magnetization and susceptibility on the BKBO single crystals at low fields in field-cooled and zero-field-cooled conditions were recorded with a superconducting quantum interference device magnetometer

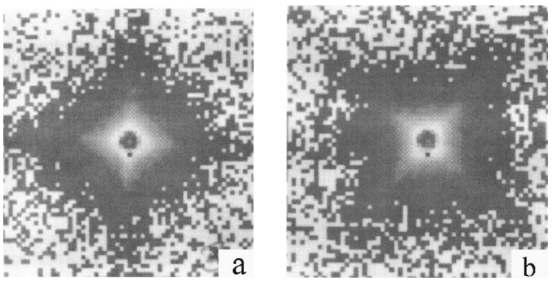

FIG. 2. The SANS patterns at two different orientations of $Ba_{0.59}K_{0.41}BiO_{3+y}$ single crystal in the (001) face: (a) x axis of the picture coincides [100] crystal direction; (b) x axis of the picture lies alone [110] crystal direction.

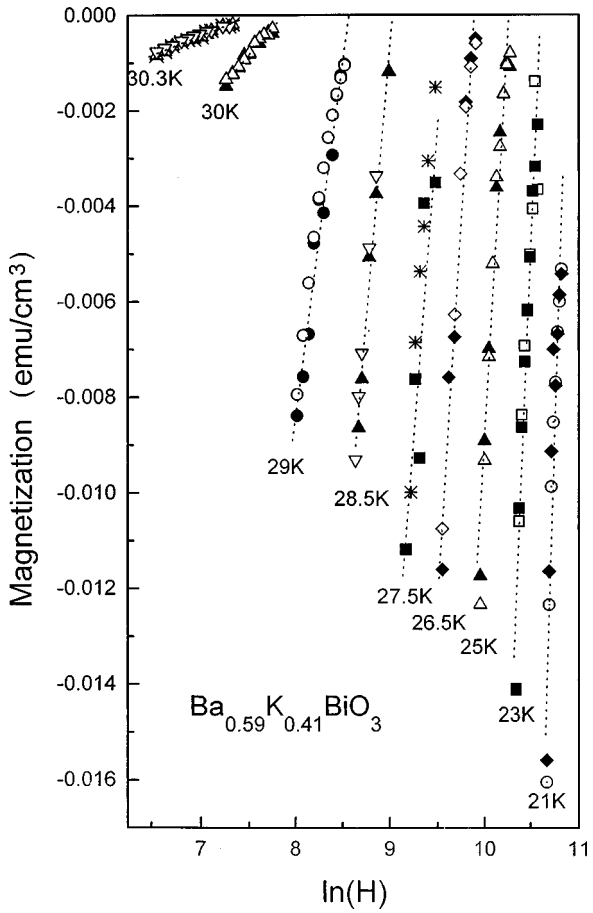

FIG. 3. Isotherms of magnetization vs the logarithm of the applied field for $Ba_{0.59}K_{0.41}BiO_{3+y}$ single crystal (open and solid symbols denote data measured at increasing and decreasing applied field, respectively).

(Quantum Design, MPMS-5) over a range of temperature 3–40 K and magnetic fields up to 50 kOe.

The susceptibility of crystals in the normal state was determined over the temperature range from 40 to 300 K in the field of 6 and 50 kOe and thereafter this contribution was subtracted from the $M(H,T)$ dependencies to pick out the magnetic response related to the superconducting state of the crystal.

III. RESULTS AND DISCUSSIONS

An analysis of hysteresis loops $M(H)$ for the BKBO single crystals with various potassium concentration show that all the measured crystals featured the peak effect on magnetization curves over a definite temperature range. The position of extra maximum on the hysteresis loops is temperature dependent, and the field of the peak effect H_p decreases with increasing temperature.

The measurements in the high field and temperature range exhibit $M(\ln H)$ dependencies that are straight lines and are successfully described by relation (1) in the field and temperature regions under investigation.

A. Reversible magnetization range

Figure 3 shows measured isotherms $M(\ln H)$ of BKBO for the $x=0.41$ crystal, which are typical for all the crystals.

TABLE II. Critical fields and Ginzburg-Landau parameters of $Ba_{1-x}K_xBiO_y$ single crystals obtained from magnetization measurements.

Critical parameter of superconductor	Composition of the single crystal		
	$Ba_{0.66}K_{0.34}BiO_3$	$Ba_{0.63}K_{0.37}BiO_3$	$Ba_{0.59}K_{0.41}BiO_3$
T_c [K (low field)]	30	29	31
H_{c2} (0) (T)	25.0	19.3	20.9
dH_{c2}/dT (T/K)	−0.78	−0.65	~0.6
$\xi(0)$ (Å)	36.4	41.5	40
λ_L (0) (Å)	~3089	~3100	3200
$\kappa(0)$	~85	~75	80
$H_{c1}(0)$ (Oe)	77	74	73
H_c (0) (T)	0.21	0.18	0.187
$\Delta C/T_c$, (mJ/mole K^2)	3.1	2.57	2.79
γ mJ/mole K^2	2.16	1.8	1.95
$N(E_F)$ (states/eV cell)	~0.46	~0.40	0.44
λ_{ph}	~1	~0.76	~0.9

The experimental data are well described by the logarithmic field dependencies in the investigated temperature range. From the same data, using relation (2), we obtained the temperature dependencies of the magnetic-field penetration depth λ_L represented in Fig. 4. Curves $\lambda_L(T)$ are well described by the classical BCS formula $\lambda_L(T)=\lambda_L(0)(1-t)^n$, where $t=T/T_c$, T_c is the superconducting transition temperature, and an exponent of $n\sim0.5$. The values $\lambda_L(0)$ as well as some other experimental and calculated parameters of superconducting single crystals are listed in Table II. As can be seen, the experimentally determined values of penetration depth $\lambda_L(0)$ for BKBO known in the literature vary from 803 to 3300 Å.[19,26,14,8,13,11,22] It must be emphasized that normal inclusions that may be present in the sample can lead to underestimating the magnetization value. Since λ_L^{-2} is proportional to the $\partial M/\partial \ln H$, the value of penetration depth λ_L can be overestimated by a constant multiplier, though the character of the temperature dependence of $\lambda_L(T)$ remains the same. But we should mention also that x-ray and neutron analysis of our crystals[57] exhibited single-phase character and a high degree of perfection of the as-grown crystals as well as practically no normal inclusions. The value of magnetic susceptibility of the crystals in the normal state, which in the high-temperature range is consistent with the data given by other authors,[10,21] verifies the single-phase structure. For this reason we have not recalculated the values of penetration depth related to the possible presence of normal ranges in crystals.

Our recent paper,[36] which deals with estimation of the temperature dependence of the upper critical magnetic field $H_{c2}(T)$ for our single crystals, reveals that near T_c, $H_{c2}(T)$ is well described by the linear relation that correlates with the Ginzburg-Landau theory. The values of $H_{c2}(0)$ and $(\partial H_{c2}/\partial T)_{T_c}$ are listed in Table II with the data. The coherence length $\xi(0)$ calculated from the relation $H_{c2}=\phi_0/2\pi\xi^2$ equals 36.4 Å ($x=0.34$), 41.5 Å ($x=0.37$), and 40 Å ($x=0.41$). With the values for $\lambda_L(0)$, we can evaluate the Ginzburg-Landau parameter values to be $\kappa=\lambda_L/\xi\sim85$ ($x=0.34$), ~75 ($x=0.37$), and 80 ($x=0.41$), respectively. We may then estimate the specific-heat jump at T_c in accordance with relation[58]

$$\Delta C/T_c=\frac{1}{8\pi g k^2}\left[\frac{\partial H_{c2}}{\partial T}\right]^2. \tag{6}$$

The Sommerfeld constant γ has been calculated through the use of the relation $\Delta C/T_c=1.43\gamma$ (Table II). As can be seen, the γ values are close to the corresponding data obtained for melted $Ba_{0.65}K_{0.35}BiO_3$ ($\gamma=2.36$ mJ/mol K^2),[8] for $Ba_{0.6}K_{0.4}BiO_3$ ($\gamma=3.4$ mJ/mol K^2) ceramic sample,[18] and

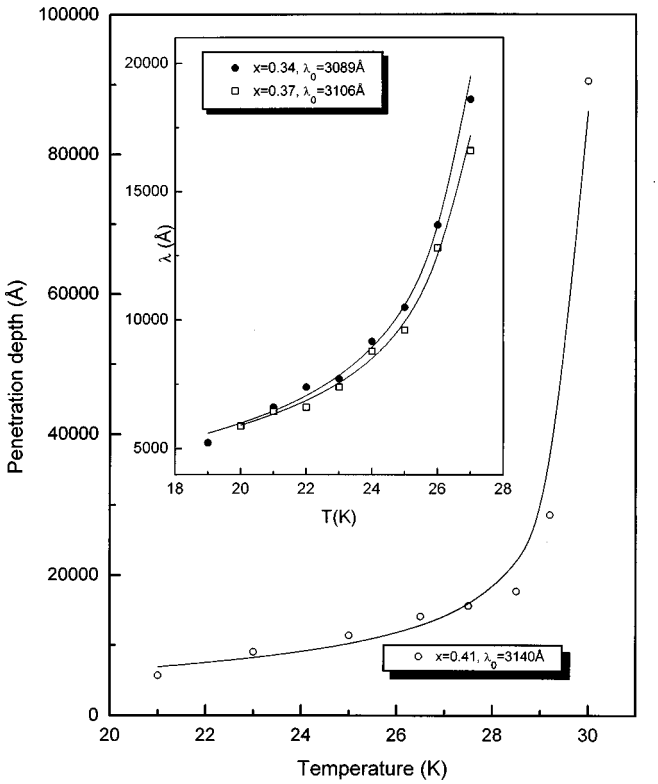

FIG. 4. Temperature dependence of the magnetic-field penetration depth for $Ba_{0.59}K_{0.41}BiO_{3+y}$ single crystal, derived on the basis of relation (2), which agrees well with the BCS formula [solid line, λ_0 (the penetration depth value at zero temperature)]. Inset: the same dependencies for $Ba_{0.66}K_{0.34}BiO_{3+y}$ and $Ba_{0.63}K_{0.37}BiO_{3+y}$ single crystals.

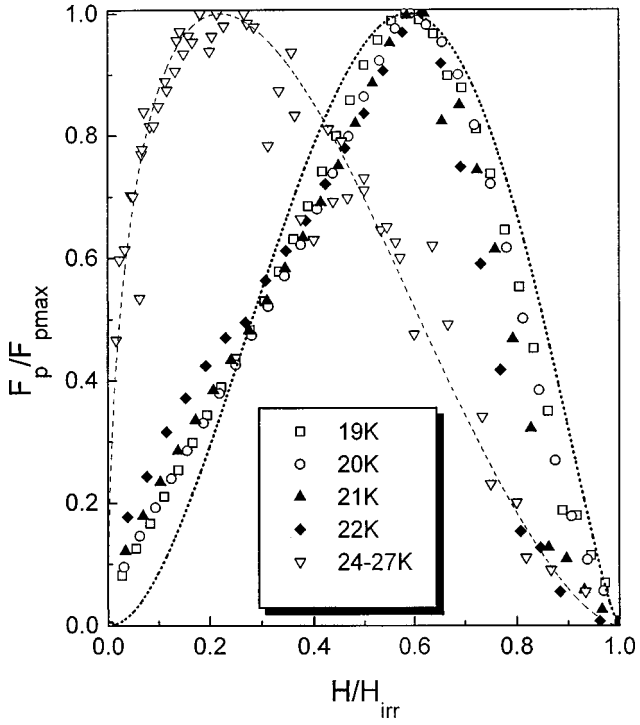

FIG. 5. The isotherms of normalized pinning force $F_p/F_{p\,\max}$ as a function of the reduced field $b=H/H_{\rm irr}$ for the $Ba_{0.66}K_{0.34}BiO_{3+y}$ single crystal. It can be seen that experimental values of reduced pinning force are satisfactorily approximated by two different curves having a peak, according to relation (5), for $b'_{\max}$ of 0.56 [2D pinning on $\Delta\kappa$ centers (dotted line)] and 0.22 [2D pinning on normal centers (dashed line)].

$Ba_{0.62}K_{0.38}BiO_3$ ($\gamma=2.31$ mJ/mol K^2) single crystal.[14] From the value of γ one can determine the resulting electron density of states at the Fermi level $N^*(E_f)$ in accordance with the expression

$$\gamma=2/3\pi^2k_B^2N^*(E_f). \tag{7}$$

The electron-phonon interaction constant $\lambda_{\rm ph}$ can also be determined from $N^*(E_f)=N(0)(1+\lambda)$, where $N(0)$ is the electron density of states of order 0.23 states/eV cell as follows from the band-structure calculations for BKBO (Ref. 59) (see Table II). The values of $\lambda_{\rm ph}\sim1$, ~0.76, and 0.9 point to the fact that the single crystals $Ba_{1-x}K_xBiO_y$ with $x=0.34$, $x=0.37$, and $x=0.41$, respectively, are superconductors with intermediate coupling.

From analysis of the magnetic susceptibility data for the BKBO single crystals in the normal state there was obtained at temperatures from 250 to 300 K the value χ is -5×10^{-5} emu/mol ($x=0.34$) and -4×10^{-5} emu/mol ($x=0.37$). In general, the magnetic susceptibility of the crystal in the normal state χ consists of several contributions[60] connected with (1) the Pauli paramagnetism χ_P; (2) the Landau diamagnetism of conduction electrons χ_L; (3) the Van Vleck paramagnetism $\chi_{\rm VV}$; (4) the electron core diamagnetism $\chi_{\rm core}$; and (5) paramagnetism of impurities $\chi_{\rm imp}$. The last contribution for BKBO crystals is very small. This is also consistent with insignificant volume of normal areas as assumed by us in the investigated crystals. The value of $\chi_L=-(m/m^*)^2\chi_p/3$ and, assuming that $m^*/m\sim7-8$ (Ref. 21)

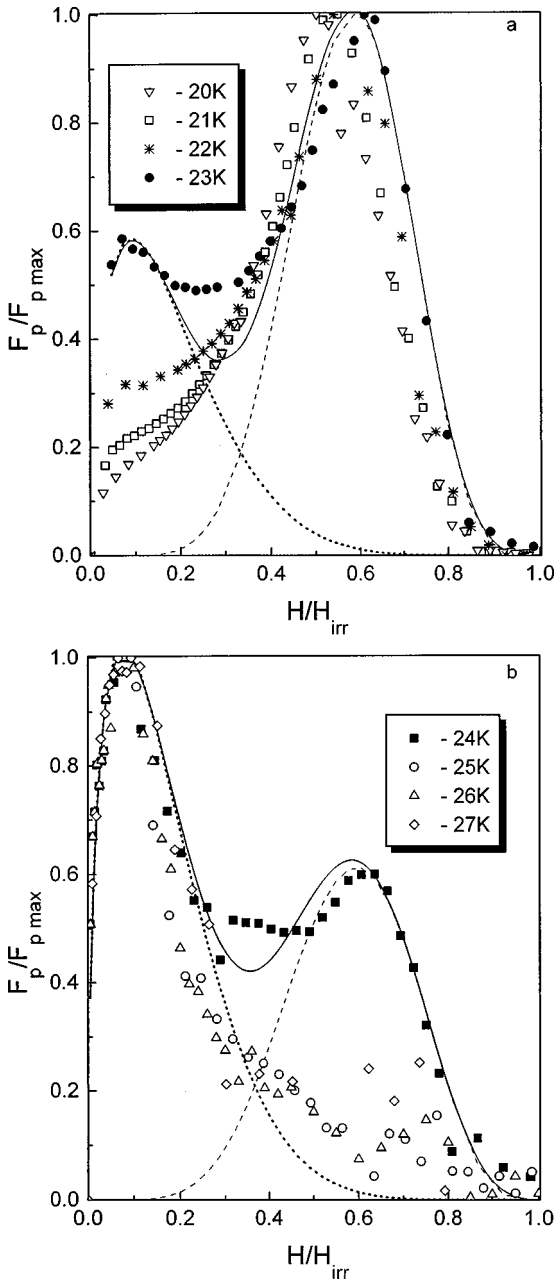

FIG. 6. (a) and (b) The isotherms of the normalized pinning force $F_p/F_{p\,\max}$ as a function of the reduced field $b=H/H_{\rm irr}$ for $Ba_{0.63}K_{0.37}BiO_{3+y}$ single crystal fitted to Eq. (5) [fittings reveals $b'_{\max}$ of 0.12 (dotted line) and 0.6 (dashed line); solid line corresponds to the sum]. As can be clearly seen, the character of vortex pinning changes drastically in $23\leqslant T\leqslant24$ K due to a type of 2D pinning-center variation.

for BKBO ($x=0.4$), the diamagnetic contribution of conduction electrons χ_L constitutes a negligibly small fraction of χ_P. The contribution of $\chi_{\rm VV}$ is also disregarded by us and the magnetic susceptibility of the BKBO single crystals becomes $\chi=\chi_P+\chi_{\rm core}$. The last value can be estimated from the tabulated values of the radii of occupied electron shells for Ba^{2+}, K^{1+}, Bi^{3+}, and O^{2-}:[61] $\chi_{\rm core}=-7.8\times10^{-5}$ emu/mol. On this basis we derive the values 2.67×10^{-5} emu/mol ($x=0.34$) and 3.7×10^{-5} emu/mol ($x=0.37$) for a contribution of the Pauli paramagnetism. The

TABLE III. List of F_p scaling low parameters for $Ba_{1-x}K_xBiO_{3+y}$ single crystals with different potassium content.

Sample no.	Potassium content x	Exponent value n	m	p	q	Exponents ratio b'_{max}	Temperature (K)
				1.95	1.52	0.56	19–22
1	0.34	0.59	1.45				
				0.48	1.70	0.22	24–28
				4.60	3.10	0.60	20–22
2	0.37	0.77	1.22				
				0.43	3.20	0.12	25–27
				0.853	8.82	0.09	
3	0.41 ($H\perp$ surface)						19–27
			1.21	2.93	6.39	0.31	
				0.78	9.8	0.07	
4	0.41 ($H\parallel$surface)						19–27
			1.21	2.96	6.58	0.31	
5	0.46	1.40	1.18	0.58	2.94	0.16	12–18

resulting density of electron states at the Fermi level is related to the Pauli susceptibility through the well-known expression

$$\chi_p = N_A(2\mu_B^2)N^*(E_f) = 2\times 0.3233\times 10^{-4}N^*(E_f), \quad (8)$$

where N_A is Avogadro's number and μ_B is the Bohr magneton. The value of the density of states $N^*(E_f)$ determined from the Pauli susceptibility in accordance with Eq. (6) is 0.42 and 0.56 states/eV cell for crystals with $x=0.34$ and $x=0.37$, respectively. Hence, the total sum of the density of states $N^*(E_f)$ calculated in terms of the specific-heat jump close to T_c (Table II) and of magnetic susceptibility in the normal state agree satisfactorily.

Earlier we have estimated by SIN tunneling measurements the superconducting gap magnitude of $2\Delta_0/k_BT \sim 4.1$,[7] which is significantly larger than the value of 3.5 for an ideal weak-linked BCS superconductor. In accordance with the Toxen empirical formula the gap and thermodynamic critical field H_c are related at low temperature by[62]

$$2\Delta_0/k_BT_c = 2T_c/H_{c0}(\partial H_c(T)/\partial T), \quad (9)$$

where Δ_0 and H_{c0} are the gap and thermodynamic critical field values at $T=0$. Note that two independent crystal characteristics, the gap and the slope of $H_c(T)$ at T_c are combined by relation (9). The right part of Eq. (9) was calculated from magnetization data to be of 4.0. The small ($\sim$2.5%) difference between SIN tunneling and calculated data allows us to determine that BKBO is not a weak-link superconductor. The relation $E_v = H_c^2H_{c1}/2H_{c2}$ also provides an estimate of the energy of vortex nucleation of $E_v/(H_c^2/8\pi) \sim 4.75\times 10^{-3}$.

B. Irreversible magnetization range

As was mentioned above, all the crystals that have been measured reveal the peak effect in magnetization curves over a broad temperature range. The temperature dependence of H_p is described well by the power law $H_p \sim (1-T/T_c)^n$. The irreversibility line $H_{irr}(T)$ is also described by the function $H_{irr}(T) \sim (1-T/T_c)^m$, though $m \neq n$. The exponents n and m vary depending on potassium content in the crystal as listed in Table III.

The analysis of the field-dependent value ΔMH (ΔM is a hysteresis loop width and $H \sim B$), proportional to the pinning force density, has revealed a similar pattern in the temperature range $T \leqslant 20$ K for all the investigated crystals. The $F_p(H)$ function goes through a maximum and shifts to a lower field range as the temperature increases, while the maximum amplitude decreases. The normalized pinning force values $F_p/F_{p\,max} = f(b^\star)$, where $b^\star = H/H_{max}$ for all the

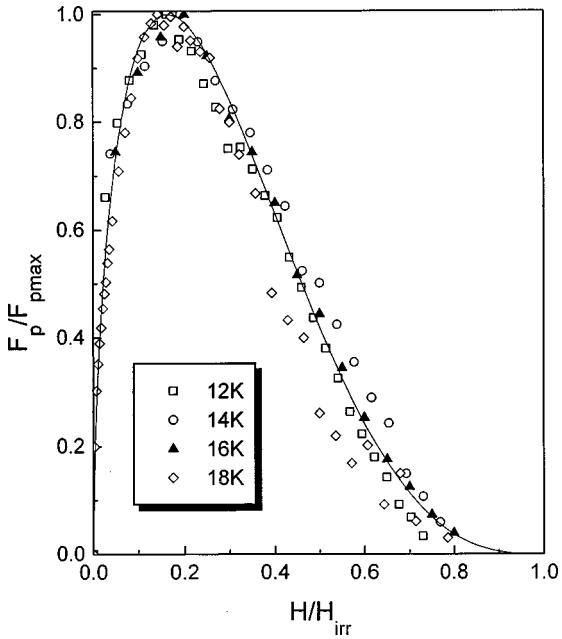

FIG. 7. The isotherms of normalized pinning force $F_p/F_{p\,max}$ as a function of the reduced field $b=H/H_{irr}$ for the $Ba_{0.54}K_{0.46}BiO_{3+y}$ single crystal scaled to a single curve by the unified pinning mechanism over the whole temperature range investigated (fitting reveals b'_{max} of 0.16 corresponding to single vortex pinning by randomly distributed 2D normal centers).

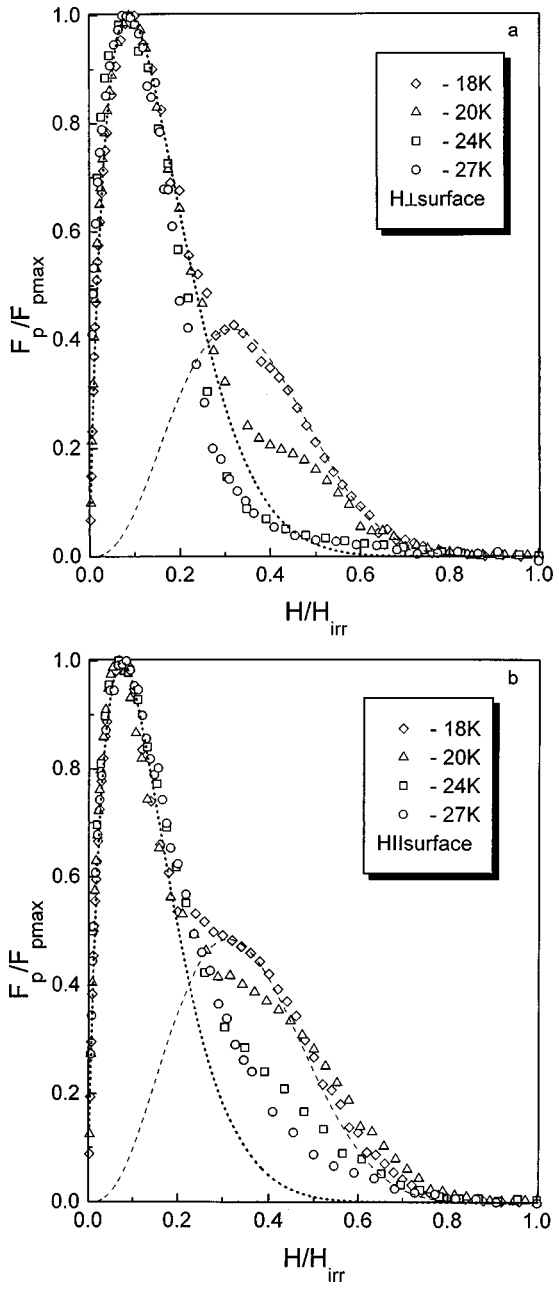

FIG. 8. The isotherms of normalized pinning force $F_p/F_{p\,\max}$ as a function of the reduced field $b=H/H_{\rm irr}$ for $Ba_{0.59}K_{0.41}BiO_{3+y}$ single crystal scaled to Eq. (10): (a) $H\perp$ the natural crystal surface [$p=0.85$, $q=8.82$ (dotted line); $p'=2.93$, $q'=6.39$ (dashed line)]; (b) $H\|$ the growth surface of crystal [$p=0.78$, $q=9.8$ (dotted line); $p'=2.96$, $q'=6.58$ (dashed line)]. The data seem to indicate, similarly as for $Ba_{0.54}K_{0.46}BiO_{3+y}$, the importance of the $\delta 1$ pinning related to the spatial variation of the charge-carrier mean free path.

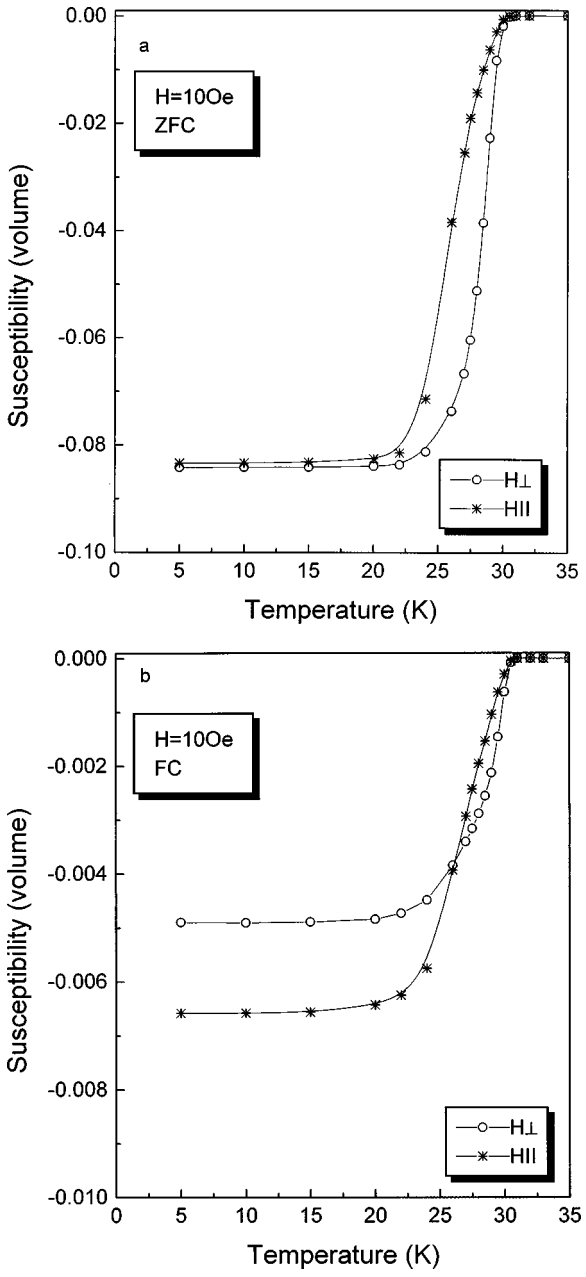

FIG. 9. Temperature dependencies of (a) the magnetic shielding (zero-field cooled) and (b) the Meissner (field cooled) signals for the $Ba_{0.59}K_{0.41}BiO_{3+y}$ single crystal (with demagnetizing factor taken in account). Field-cooled Meissner susceptibility is distinctly different for both field orientations in the whole temperature range indicating a stronger pinning in low fields for $H_\perp$.

crystals are aligned with one curve up to $H_{\max}$ (see, for example, Ref. 36). For temperatures $T>23$ K near T_c, though, the deviation from the single asymptotic behavior in the whole magnetic field range is clearly seen. For instance, compounds with $x=0.34$, 0.37 tend to change the character of dependence as the temperature rises from a curve with a narrow peak to a curve with a broader one.

The normalized pinning force density of the investigated BKBO crystals yielded via expression (5) the scaling parameters that are listed in Table III. Examples of fitted curves are presented in Figs. 5–8. It is well known that $p<q$ for conventional hard superconductors, as well as for copper-containing HTSC $YBa_2Cu_3O_{7-\delta}$ (YBCO),[43,51] BiSrCaCuO,[52] and TlBaCuO.[53] In our case this condition is satisfied with the BKBO single crystals of potassium content $x=0.41$ ($T=19-27$ K), $x=0.46$ ($T=12-18$ K), but for $x=0.34$ and 0.37 at temperatures close to T_c only. The condition $p<q$ is in agreement with the concept of the critical shear strength of the flux lattice introduced by Kramer.[41] However, in the lower temperature range the relation $p>q$ was obtained for

crystals with $x=0.34$ and 0.37 (Figs. 5 and 6). As could be clearly seen in Figs. 6(a) and 6(b), the character of vortex pinning changes drastically at $T\leqslant 23$ K for the sample with $x=0.37$.

It is recognized[40] that the peak positions on $F_p/F_{p\,\max}=f(b')$ curves point out to the pinning mechanism and could be determined as $b'_{\max}=p/(p+q)$. The $b'_{\max}$ values for crystals with different composition are also summarized in Table III. From Figs. 5 and 6, in accordance with the above-mentioned model, one can make an assumption for crystals with $x=0.34$ and 0.37 about (i) the character of the pinning centers being two dimensional (2D); (ii) two different types of pinning centers (normal and $\Delta\kappa$); (iii) the peak effect being due to the crossover between at least two different pinning mechanisms induced by external magnetic field and/or temperature.

For the BKBO single crystals with $x>0.33$, as established in Ref. 36, the peak effect exists though no exhaustive explanation has been provided. In the YBCO and BiSrCaCuO systems the peak effect occurs but has a different interpretation. Thus in the case of YBCO the peak effect is accounted for by employing (i) the model of superconductivity depression by a magnetic field in oxygen-deficient ranges that become the pinning centers[63] or (ii) the model of crossover from the single to collective flux creep leading to the reduction of magnetization relaxation in intermediate fields.[64] The matching effect has been proposed in Ref. 65 to explain the peak effect in BiSrCaCuO. The peak effect in Tl-based single crystals is related to the softening of the vortex lattice making for the pinning efficiency with plausible 3D to 2D transition or melting of the 3D lattice; in this instance the anisotropy of electronic properties $\gamma=(m_c^\star/m_{ab}^\star)^{1/2}$ is favored.

The findings for scaling law for the bulk pinning force in cubic single crystals of BKBO with various potassium concentration indicate that the peak effect in crystals with $x=0.34$ and 0.37 is related to the crossover of two pinning mechanisms as the magnetic field increases. At the same time our observation of the scaling behavior of the crystal with $x=0.46$ (Fig. 7) is well described by the unified pinning mechanism over the whole temperature range investigated. From our earlier study on the same sample, the dependence of the relaxation rate value of $S(H)$ at different temperatures has been plotted. The $S(H)$ peaks on the isotherms were observed for $H\sim 0.5H_p$ (H_p marks the peak-effect field).[36] These data contradict the suggestion that dimensional crossover between 3D and 2D vortex stricture causes the peak effect in the sample. The detailed analysis with the prediction of the theoretical models describing so-called δT_c and $\delta 1$ pinning[65] revealed a conclusion that the single-vortex pinning by randomly distributed 2D normal centers occurs in the crystal with $x=0.46$.

C. Seeded growth-induced anisotropy and pinning centers for $Ba_{0.59}K_{0.41}BiO_{3+y}$

The first indication in microstructure evidence to indicate what might be responsible for the pinning is presented below. As have been mentioned, the sample with $x=0.41$ reveals the seeded growth-induced anisotropy. The stripe

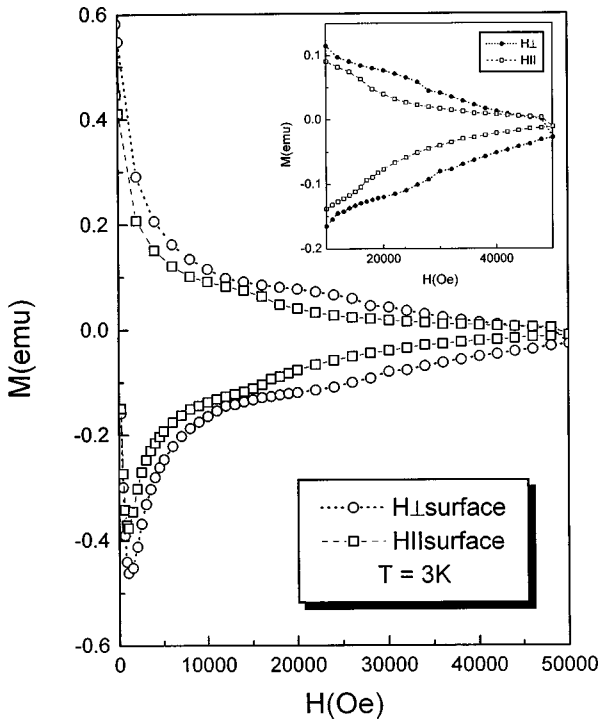

FIG. 10. Volume magnetization hysteresis loops for two different orientations of the field to the natural growth surface of $Ba_{0.59}K_{0.41}BiO_{3+y}$ single crystal. Inset: for better presentation of peak effect, the low-field region is omitted.

structure of defects oriented parallel to the natural growth surface of crystal has a period approximately of 1 μm (Fig. 1).

The critical temperature T_c as obtained from the extrapolation of the maximum slope of $\chi(T)$ to χ_0, determined from $\chi(T)$ after zero-field cooling in an applied field of 10 Oe, is equal to 30.5 K (Fig. 9). This value is greater than those observed previously for BKBO ($x=0.34$, 0.37, and 0.46) crystals.[35] Such a value of T_c indicates that the oxygen concentration is close to the optimal one [$y\approx -0.05$ (Ref. 66)]. The shielding effect in $H_{\rm ext}=10$ Oe is close to ideal of $1/4\pi$ taking into account a demagnetizing factor. The anisotropy in the zero-field-cooled data is reflected only in some differences in the transition region [Fig. 9(a)]. The field-cooled Meissner susceptibility is distinctly different for both field orientations in the whole temperature range [Fig. 9(b)], indicating stronger pinning in low fields in the case of the external field oriented perpendicular to the natural growth surface of crystal ($H_\perp$). On hysteresis loops a relatively weak peak effect was observed in the low-temperature range of 3–7 K. The position of the peak depends on the field orientation (Fig. 10) being shifted to higher fields for $H_\perp$. The width of hysteresis loop ΔM behaves as follows: (a) the ratio of $\Delta M(H_\perp)/\Delta M(H_\parallel)$ is a function of temperature and magnetic field, but its maximal value (1.9–2.3) is practically independent of temperature in the range of 3–27 K. The position of this maximum shifts from higher to lower fields with increasing temperature. It changes from a broad maximum (in the range from 25 up to 48 kOe) at low T (3–7 K) to a somewhat complicated structure in small fields up to 1.5 kOe at 27 K [Figs. 11(a), 11(b), and 11(c)]; (b) at temperature of $T=3-18$ K, in the entire field range $H\leqslant 50$ kOe the

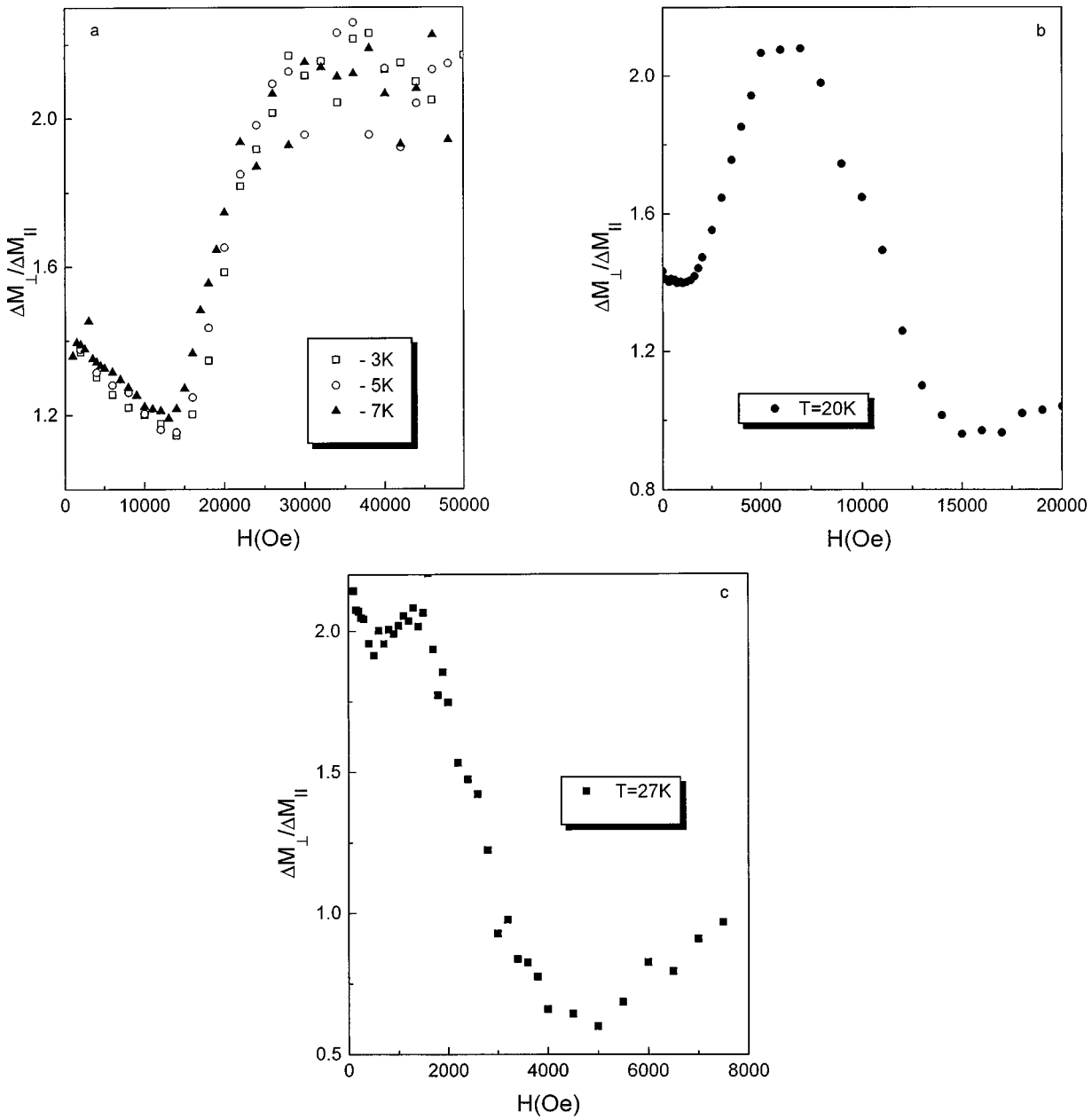

FIG. 11. (a), (b), and (c) Ratio $\Delta M(H_\perp)/\Delta M(H_\parallel)$ as a function of external magnetic field for several temperatures. It should be underscored that the condition $\Delta M(H_\perp)/\Delta M(H_\parallel)>1$ is fulfilled except in the higher-field region at $T\geqslant 20$ K in the rest of the H-T range investigated.

value of $\Delta M(H_\perp)/\Delta M(H_\parallel)$ is larger than 1; (c) at 20 K and $H\geqslant 14$ kOe the ratio is close to 1; (d) at higher temperatures ($T>20$ K) and magnetic fields ($14\ \text{kOe}\leqslant H\leqslant H_{\text{irr}}$) the ratio is less than 1 (reaching a minimum of about 0.6). The irreversible magnetization anisotropy is clearly seen to be the opposite character of $\Delta M(H)$ curves cross sections under small and high external fields (Fig. 12). It should be emphasized that the condition $\Delta M(H_\perp)/\Delta M(H_\parallel)>1$ is fulfilled except in the higher-field region, at $T\geqslant 20$ K. This could be explained by taking into account the chemical etching experiments. The results could be understood assuming that during the seeded growth of crystal some kind of macroscopic layered structure was formed (with a period of 1–2 μm, or even smaller, not detected by chemical etching technique we used), which is responsible for an anisotropy of critical current. The interlayer borders play two different roles in the case of magnetic field oriented parallel to the natural surface ($H_\parallel$): first of all, they act as weak links limiting the critical current density and second they act as two-dimensional pinning centers. Weak links are responsible for the ratio $\Delta M(H_\perp)/\Delta M(H_\parallel)>1$ in the majority of H-T space, whereas an existence of natural 2D pinning centers plays a significant role in the higher-field region at $T\geqslant 20$ K resulting in $\Delta M(H_\perp)/\Delta M(H_\parallel)<1$. Because the effectiveness of both mechanisms depends differently on temperature and magnetic field, this leads to a complicated dependence of the ratio versus H and T (Fig. 11).

Simultaneously, some part of oxygen defects can be ordered along the direction normal to the natural surface as an effect of the application of an electric field of this direction

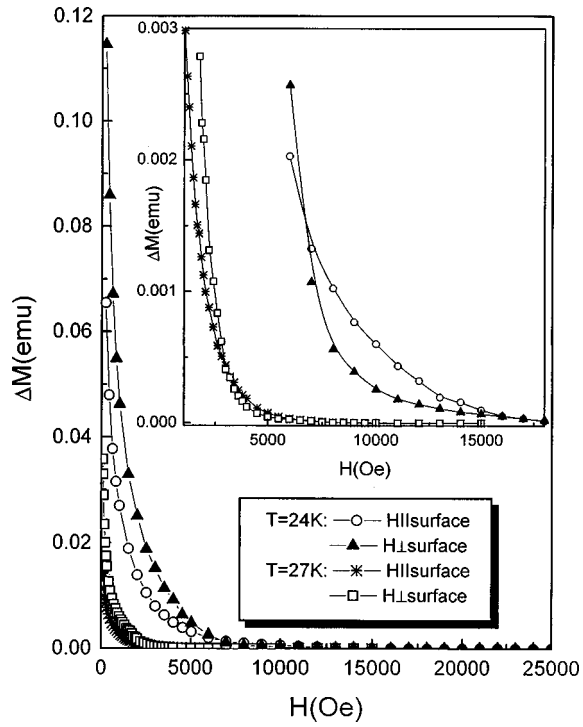

FIG. 12. The irreversible magnetization anisotropy for different external-field orientations to the natural surface for the $Ba_{0.59}K_{0.41}BiO_{3+y}$ single crystal grown on a seed. Inset: the opposite character is clearly seen for $\Delta M(H)$ curves cross section under small and high external fields.

during the crystal growth process. The presence of such rather low dimensional defects, which can be effective as pinning centers in low magnetic field of orientation $H_{\perp}$, could be responsible for the difference in field-cooled susceptibility [Fig. 9(b)]. It has been found that the changes of the pinning force (or rather its main contribution) with external magnetic field and temperature can be well described by the universal scaling law

$$F_p/F_{p\ \max}=Ab^{p1}(1-b)^{q1}+Bb^{p2}(1-b)^{q2}, \qquad (10)$$

where $b=H/H_{\rm irr}$ [Figs. 8(a) and 8(b)]. The obtained results (Table III) seem to indicate, similarly as for BKBO ($x=0.46$), the importance of the depinning related to the spatial variation of charge-carrier mean free path.

The observed peak effect seems to be caused by a variation of the δl-pinning character due to a sharp change of pinning center geometry from a surface to a point with decreasing temperature.

It was found that in the limit of the estimation of errors $H_{\rm irr}$ does not depend on the field orientation. In the temperature range of 18–27 K, where the irreversibility field could be estimated, $H_{\rm irr}$ displays a power law of the reduced temperature (T/T_c) according to the relation $H_{\rm irr}=132(1-T/30.5)^{1.21}$ kOe. The reversible part of magnetization curves is identical for both applied-field orientations, which indicates the isotropy of penetration depth under these temperatures.

IV. CONCLUSIONS

We analyzed the reversible and irreversible magnetization near T_c for $Ba_{1-x}K_xBiO_{3+y}$ single crystals with different potassium content. The isotherms of reversible magnetization were used to estimate the most important characteristics of the superconductors with a cubic structure. The values of the electron-phonon interaction constant of $\lambda_{\rm ph}\sim 1$, ~ 0.76, and 0.9 for $Ba_{1-x}K_xBiO_{3+y}$ with $x=0.34$, $x=0.37$, and $x=0.41$, respectively, have been obtained. The data show that the family belongs to oxide superconductors with at least intermediate strength of coupling.

It could be concluded now, from the irreversible magnetization data analysis, that pinning in cubic BKBO is caused by an interaction between either the flux-line lattice or individual vortices and the microstructure of the superconductor. The microstructure provides some spatial variation of the basic superconducting properties, and thus the strength of the pinning is related to the basic superconductivity, and therefore involves the thermodynamic critical field. For true pinning the scaling must be to the thermodynamic critical field, which, in turn, can, via κ, be related to the upper critical field H_{c2}. If the pinning force is defined by the moment at which the flux breaks away from the pinning centers, then the scaling for the oxide superconductor will follow relation (5). If the flux lattice begins to shear, whether by the dislocation mechanism Dew-Hughes proposed,[40] or by some other means, the critical Lorentz force is related to the properties of the flux-line lattice, and in particular, the elastic constants of the lattice. These usually show something that approximates $F_p\sim b^{1/2}(1-b)^2$ and it is not unreasonable that in HTSO they might scale to the irreversibility field, i.e., $b=B/B_{\rm irr}$, as this is the field at which the lattice constants go to zero. If we now look at our results, those for $x=0.46$ (Fig. 7) clearly indicate that at all temperatures the flux is so strongly pinned (by the unified pinning mechanism over the whole temperature range investigated) that the lattice shears before unpinning. This is also the case for the other three compositions at temperatures near T_c. The curves at the lower temperatures could scale as those that drive relation (5) if the reduced field were related to B_{c2} rather than the lower $B_{\rm irr}$, with a cutoff as $B_{\rm irr}$ is approached. This requires a mechanism whereby the flux is pinned at lower temperatures with a pinning strength less than the shear strength of the lattice, but which changes with temperature less sharply than does the lattice shear strength so that at high temperatures the lattice shears before it unpins. We can assume that such changes take place in BKBO ($x=0.41$) with a high probability. In particular, the observed peak effect seems to be caused by a variation of the δl pinning character due to sharp change of pinning centers geometry from 2D to a point with decreasing temperature. From the data obtained we can conclude for crystals with $x=0.34$ and 0.37 that (i) there is 2D geometry of the pinning centers in all the temperature range observed; (ii) there are two different types of pinning centers (normal and $\Delta\kappa$); (iii) the peak effect is due to the crossover between δl and δT_c pinning mechanisms induced by external magnetic field and/or temperature.

ACKNOWLEDGMENTS

The work in Minsk and Maryland was supported in part by the CRDF program, Grant No. BP 1-111 and in Warsaw by the Polish State Committee for Scientific Research under Contract No. 2P30211407.

[1] J. Bardeen, L. N. Cooper, and J. R. Schiffer, Phys. Rev. **106**, 162 (1957).
[2] Q. Huang, J. F. Zasadzinski, N. Tralshawala, K. E. Gray, D. G. Hinks, J. L. Peng, and R. L. Greene, Nature (London) **347**, 369 (1990).
[3] H. Sato, H. Takagi, and S. S. Uchida, Physica C **169**, 391 (1990).
[4] B. M. Moon, C. E. Platt, R. A. Schweinfurth, and D. J. Van Harlingen, Appl. Phys. Lett. **59**, 1905 (1991).
[5] J. F. Zasadzinski, N. Tralshawala, D. G. Hinks, B. Dabrowski, A. N. Mitchell, and D. R. Richards, Physica C **158**, 519 (1989).
[6] F. Sharifi, A. Pargellis, R. C. Dynes, B. Miller, E. S. Hellman, J. Rosamilia, and E. H. Hartford, Phys. Rev. B **44**, 12 521 (1991).
[7] P. Samuely, N. L. Bobrov, A. G. M. Jansen, P. Wyder, S. N. Barilo, and S. V. Shiryaev, Phys. Rev. B **48**, 13 904 (1993).
[8] H. C. Jang, M. H. Hsieh, D. S. Lee, and H. E. Horng, Phys. Rev. B **42**, 2551 (1990).
[9] M. Affronte, J. Marcus, C. Escribe Filippini, A. Sulpice, H. Rakoto, J. M. Broto, J. C. Ousset, S. Askenazy, and A. G. M. Jansen, Phys. Rev. B **49**, 3502 (1994).
[10] B. Batlogg, R. J. Cava, L. W. Rupp, A. M. Mujsce, J. J. Krajewski, J. P. Remeika, W. F. Peck, A. S. Cooper, and G. P. Espinosa, Phys. Rev. Lett. **61**, 1670 (1988).
[11] Z. I. Huang, H. H. Fang, Y. Y. Hue, P. H. Hor, C. W. Chu, M. L. Norton, and H. Y. Tang, Physica C **180**, 331 (1991).
[12] V. F. Gantmakher, L. A. Klinkova, N. V. Barkowskii, G. E. Tsadynzhapov, S. Wieger, and A. K. Geim, Phys. Rev. B **54**, 6133 (1996).
[13] W. K. Kwok, U. Welp, G. Crabtree, K. G. Vandervoort, R. Hulsher, Y. Zheng, B. Dabrowski, and L. G. Hinks, Phys. Rev. B **40**, 9400 (1989).
[14] T. Uchida, S. Nakamura, N. Suzuki, Y. Nagata, W. D. Mosley, M. D. Lan, P. Klavins, and R. N. Shelton, Physica C **215**, 350 (1993).
[15] R. A. Schweinfurth, C. E. Platt, M. R. Teepl, and D. J. van Harlingen, Appl. Phys. Lett. **61**, 480 (1992).
[16] Z. Schlesinger, R. T. Collins, J. A. Calise, D. G. Hinks, A. W. Mitchell, Y. Zheng, B. Dabrowski, N. E. Bickers, and D. J. Scalapino, Phys. Rev. B **40**, 6862 (1989).
[17] J. E. Graebner, L. F. Schneemeyer, and J. K. Thomas, Phys. Rev. B **39**, 9682 (1989).
[18] S. E. Stupp, M. E. Reeves, D. M. Ginsberg, D. G. Hinks, B. Dabrowski, and K. G. Vanderviirt, Phys. Rev. B **40**, 10 878 (1989).
[19] M. S. Pambianchi, S. N. Anlage, E. S. Hellman, E. H. Hartford, M. Bruns, and S. Y. Lee, Appl. Phys. Lett. **64**, 244 (1994).
[20] A. I. Liechtenstein, I. I. Mazin, C. O. Rodriguez, O. Jepsen, O. K. Andersen, and M. Methfessel, Phys. Rev. B **44**, 5388 (1991).
[21] G. K. Panova, A. A. Schikov, B. I. Savel'ev, A. P. Zhernov, N. V. Anschukova, A. I. Golovaschkin, A. I. Ivanova, and A. P. Rusakov, Zh. Éksp. Teor. Fiz. **103**, 605 (1993) [JETP **75**, 478 (1993)].
[22] S. N. Barilo, V. I. Gatalskaya, D. I. Zhigunov, L. A. Kurochkin, and S. V. Shiryaev, Supercond., Phys. Chem. Technol. **7**, 753 (1994).
[23] G. Zhao and D. E. Morris, Phys. Rev. B **51**, 12 848 (1995).
[24] T. J. Ansaldo, Z. R. Wang, J. H. Cho, D. C. Johnston, and T. M. Riseman, Physica C **185–189**, 1889 (1991).
[25] M. Kosuji, Z. Akimitsu, T. Uchida, M. Furuja, J. Nagata, and T. Ekino, Physica C **229**, 389 (1994).
[26] V. F. Gantmaker, L. A. Klinkova, A. M. Neminskii, and M. V. Filatova, Zh. Éksp. Teor. Fiz. **101**, 1612 (1992) [Sov. Phys. JETP **74**, 859 (1992)].
[27] J. P. Carbotte, Rev. Mod. Phys. **62**, 1027 (1990).
[28] D. G. Hinks, D. R. Richards, B. Dabrowski, D. T. Marx, and A. N. Mitchell, Physica C **162–164**, 1405 (1989).
[29] C. R. Loong, Phys. Rev. Lett. **66**, 3217 (1991).
[30] Sh. Pei, J. D. Jorgensen, B. Dabrowski, D. G. Hinks, D. R. Richards, A. W. Mitchell, J. M. Newsam, S. K. Sinha, D. Vaknin, and A. J. Jacobson, Phys. Rev. B **41**, 4126 (1990).
[31] O. Navarro, Physica C **265**, 73 (1996).
[32] V. S. Kogan, M. M. Fang, and S. Mitra, Phys. Rev. B **38**, 11 958 (1988).
[33] S. Mitra, J. H. Cho, W. C. Lee, D. C. Johnston, and V. G. Kogan, Phys. Rev. B **40**, 2674 (1989).
[34] V. G. Kogan, M. Ledvij, A. Yu. Simonov, J. H. Cho, and D. C. Jonston, Phys. Rev. Lett. **70**, 1870 (1993).
[35] G. Blatter, M. V. Feigelman, V. B. Geshkenbein, A. I. Larkin, and V. M. Vinokur, Rev. Mod. Phys. **66**, 1125 (1994).
[36] H. Szymczak, M. Baran, R. Szymczak, S. N. Barilo, V. I. Gatalskaya, and S. V. Shiryaev, SPIE Proc. **3178**, 262 (1997); S. N. Barilo, V. I. Gatalskaya, S. V. Shiryaev, M. Baran, H. Szymczak, and R. Szymczak, Fiz. Nizk. Temp. **23**, 159 (1997) [Sov. J. Low Temp. Phys. **23**, 116 (1997)]; M. Baran, H. Szymczak, R. Szymczak, S. N. Barilo, V. I. Gatalskaya, and S. V. Shiryaev, J. Magn. Magn. Mater. **166**, 124 (1997).
[37] A. M. Campbell, J. E. Evetts, and D. Dew-Hughes, Philos. Mag. **18**, 313 (1968).
[38] W. A. Fietz and W. W. Webb, Phys. Rev. **178**, 969 (1969).
[39] A. M. Campbell and J. E. Evetts, Adv. Phys. **21**, 199 (1972).
[40] D. Dew-Hughes, Philos. Mag. **30**, 293 (1974).
[41] E. D. Kramer, J. Appl. Phys. **44**, 1360 (1973).
[42] K. Kishio, Y. Nakayama, N. Notohira, T. Noda, T. Kobayashi, K. Kitazawa, K. Yamafuji, I. Tanaka, and H. Kojima, Supercond. Sci. Technol. **5**, 569 (1992).
[43] T. Kobayashi, T. Kimurea, J. Shimoyama, K. Kishio, K. Kitazawa, and K. Yamafuji, Physica C **254**, 213 (1995).
[44] J. M. Li, F. R. deBoer, L. W. Roeland, M. J. V. Menken, K. Kadowaki, A. A. Menovsky, J. J. M. Franse, and P. H. Kes, Physica C **169**, 81 (1990).
[45] H. Theuss and H. Kronmuller, Physica C **177**, 253 (1991).
[46] R. Wördenweber, K. Heinemann, G. V. S. Sastry, and H. C. Freyhardt, Cryogenics **29**, 458 (1990).
[47] L. Civale, M. W. McElfrech, A. D. Marwick, F. Holtzberg, C. Felid, J. R. Thompson, and D. K. Christen, Phys. Rev. B **43**, 13 732 (1991).
[48] R. Hiergeist, R. Hergt, A. Erb, H. G. Schnack, and R. Grissen, Physica C **235–240**, 2743 (1994).
[49] M. Xu, D. K. Finnemore, K. Zhang, B. Dabrowski, G. W. Crabtree, and D. G. Hinks, in *Proceedings of the Seventh International Workshop on Critical Currents in High Temperature Superconductivity, Alpbach, 1994*, edited by H. W. Weber (World Scientific, Singapore, 1994), p. 323.
[50] L. Klein, E. R. Yacoby, Y. Yeshurun, A. Erb, G. Muller-Vogt, V. Breit, and H. Wuhl, Phys. Rev. B **49**, 4403 (1994).
[51] H. Kumakura, K. Togano, N. Tomita, E. Yanagisawa, S. Okayasu, and Y. Kazumata, Physica C **251**, 231 (1995).
[52] R. Prozorov, A. Tsameret, Y. Yeshurun, G. Koren, M. Konczykowski, and S. Bouffard, Physica C **234**, 311 (1994).
[53] R. A. Rose, S. B. Ota, P. A. J. de Grovt, and B. Jayaram, Physica C **170**, 51 (1990).

[54] J. Y. Yuang, S. J. Wang, T. M. Uen, and Y. S. Gou, Phys. Rev. B **46**, 1188 (1992).
[55] L. Niel, Cryogenics **321**, 975 (1992).
[56] S. N. Barilo, D. I. Zhigunov, L. A. Kurochkin, A. V. Pushkarev, and S. V. Shiryaev, Sverkhprovodimost: Fiz. Khim. Tekh. **5**, 1084 (1992) [Sov. Phys. Supercond. **5**, 1081 (1992).
[57] S. N. Barilo, N. M. Olekhnovich, N. S. Orlova, A. V. Pushkarev, A. N. Salak, and S. V. Shiryaev, Cryst. Res. Technol. **31**, 107 (1996).
[58] R. R. Hake, Phys. Rev. **166**, 471 (1968).
[59] L. F. Mattheiss and D. R. Hamann, Phys. Rev. Lett. **60**, 2681 (1988).
[60] A. K. Gandopadhyay and J. S. Schilling, Physica C **264**, 281 (1996).
[61] *Tablitsy Fizitheskikh Velithin*, edited by I. K. Kikoin (Atomizdat, Moscow, 1976), p. 302.
[62] A. M. Toxen, Phys. Rev. Lett. **15**, 462 (1965).
[63] M. Dauemling, J. M. Seunjens, and D. Larbalestver, Nature (London) **346**, 332 (1990).
[64] N. Chikumoto, M. Konczykowski, N. Notohira, and A. P. Malozemoff, Phys. Rev. Lett. **69**, 1260 (1992).
[65] P. N. Kes and J. Van den Berg, in *Studies of High Temperature Superconductors*, edited by A. V. Narlikar (Nova Science, New York, 1990), Vol. 5, p. 83.
[66] Y. Idemoto, Y. Iwata, and K. Fueki, Physica C **222**, 257 (1994).